Arterial blood contrast (ABC) enabled by magnetization transfer (MT): a novel MRI technique for enhancing the measurement of brain activation changes

Jenni Schulz[*1], Zahra Fazal[*1], Riccardo Metere[1], José P. Marques[1], and David G. Norris[1,2,3]

[1]Donders Institute for Brain, Cognition and Behaviour, Radboud University Nijmegen, Nijmegen, Netherlands

[2]Erwin L. Hahn Institute for Magnetic Resonance Imaging, University Duisburg-Essen, Essen, Germany

[3]Magnetic Detection and Imaging, Science and Technology Faculty, University of Twente

[*]Contributed equally.

Abstract

Functional brain imaging in humans is almost exclusively performed using blood oxygenation level dependent (BOLD) contrast. This typically requires a period of tens of milliseconds after excitation of the spin system to achieve maximum contrast, leading to inefficient use of acquisition time, reduced image quality, and inhomogeneous sensitivity throughout the cortex. We utilise magnetisation transfer to suppress the signal differentially from grey matter relative to blood, so that the local increase in blood volume associated with brain activation (mainly occurring in the arterioles and capillaries) will increase the measured signal. Arterial blood contrast (ABC) is additive to the residual BOLD effect, but will have its maximum value at the time of excitation. We measured brain activation using combined ABC and residual BOLD contrast at different times post-excitation and compare this to standard BOLD. We conclude that using ABC and measuring shortly after excitation gives comparable sensitivity to standard BOLD but will provide greater efficiency, spatial specificity, improved image quality, and lower inter-subject variability. ABC offers new perspectives for performing functional MRI.

Introduction

Brain activation studies conducted using functional magnetic resonance imaging (fMRI) have made an enormous contribution to our understanding of the biological underpinnings of human cognition and behaviour, as well as having a broader societal impact, ranging from pre-operative planning, diagnosis, to improved understanding of mental illnesses and neurological disorders.[1]

fMRI typically uses Blood Oxygenation Level Dependent (BOLD) contrast whereby paramagnetic deoxyhemoglobin acts as an endogenous contrast agent.[2] Upon brain activation, local changes in blood flow (CBF), -volume (CBV), and metabolic rate lead to a reduction in deoxyhemoglobin concentration and a corresponding increase in the transverse relaxation time. The resultant signal changes are measured most commonly with a gradient-echo echo planar imaging (GE-EPI) sequence. For optimum sensitivity, the echo time (TE) should match the transverse relaxation time of the tissue, typically some tens of milliseconds. This technique has the following disadvantages: First, the relatively long TE limits the efficiency, reduces the signal intensity by a factor of about three, and makes the method prone to artefacts, particularly signal dropout in regions of poor static main field homogeneity. Second, reliance on changes in deoxyhaemoglobin concentration in the capillaries and post-capillary vessels has the consequence that the measured activation will always be downstream of the underlying neuronal activity. Third, the sensitivity will vary through the brain with the local value of the transverse relaxation time.

Recently there has been increasing interest in measuring brain activation by using techniques based on changes in CBV,[3-11] which is known to be better localised to the source of neuronal activity than BOLD.[12, 13] One approach to sensitise the MRI signal to changes in blood volume is to use magnetisation transfer to differentially attenuate the signal from tissue, while that from blood is largely unaffected.[14, 15] An increase in blood volume, such as that occurring as a result

of brain activation, will lead to an increase in signal intensity.[16-18] Early applications of MT, in conjunction with brain activation studies, explored the effect of MT on BOLD-contrast,[19, 20] or exploited MT effects to measure blood volume.[16, 18] These experiments used lengthy off-resonance pulses of several seconds duration and TEs similar to those used in standard BOLD imaging.

Here, we diverge from previous approaches by using on-resonance pulsed MT[21] and minimising TE. Pulsed MT efficiently saturates tissue signal,[21] increasing the sensitivity to changes in blood volume, which will be highest at TE=0. The origin of blood volume changes has been analysed by Krieger et al., who ascribe percentage volume changes of 60%, 30%, and 10% to the arterial, capillary, and venous compartments, respectively.[22] Furthermore, Cai et al. [23] showed that the magnetisation transfer ratio (MTR) is higher for venous than for arterial blood. Water exchange between the tissue and capillaries will also diminish the venous contribution when the tissue signal is partially saturated by MT.[17] These two effects will further reduce the relative contribution of the venous compartment to the MT-induced signal change. We can thus expect more than 60% of the MT-weighted signal variation at TE=0 to come from arterioles, and less than 10% from the venous compartment. At rest, it has been shown that most oxygen exchange occurs in the smallest arterioles, and in the first branches of the capillary bed.[24] Upon activation, the increases in arterial and capillary blood volume will lead to increased flow and perfusion, as well as oxygen exchange occurring more evenly throughout the capillary bed. If we suppress the tissue signal using MT, then we can expect an increase in the total signal to occur because of increased blood volume, but also because of an increase in the blood oxygenation level within the capillaries. For these reasons, we have elected to term the additional functional contrast generated by suppression of grey matter signal ‘arterial blood contrast’ (ABC).

One fortunate characteristic of ABC contrast is that it is additive to the BOLD response, as an increase in brain activity will lead to an increase in both signals. With ABC, the signal increase

can be ascribed to an increase in the magnetisation within a voxel. Whereas with BOLD, the signal increases are caused by an increase in the transverse relaxation time. To estimate a pure ABC signal change, it would be necessary to perform an experiment at zero TE, which is technically challenging, especially within the constraints of a realistic fMRI experiment. We can expect, however, that the introduction of ABC will modify the activation recorded at short TEs. In this work, we used a multi-echo gradient-echo echo-planar imaging (EPI) pulse sequence with and without MT applied to acquire data over a range of TE-values. The two experiments are referred to as MT-on and MT-off, with the TE for data acquired at a given TE denoted in subscript, *e.g.,* MT-on$_{TE=6.9}$ for the first echo of the MT-on acquisition. By keeping all other parameters constant between the two datasets, we explored whether the application of MT improves the sensitivity to activation at short TE, and compared this to the BOLD response. Specifically, the images from the MT-on experiment can be expected to have an ABC that will decay exponentially with TE, and a BOLD contribution (reduced because of the reduction in grey matter signal) that will increase with TE. The MT-off experiment will display the classic BOLD signal dependence on TE,[25] with full BOLD sensitivity.

Results

Data were obtained from 16 subjects using a simple visual stimulus paradigm, pre-processed using standard fMRI analysis tools, and a first level statistical analysis was performed (*c.f.* Methods). Group level activation maps were obtained using mixed-effect statistics. Figure 1 shows how the activation patterns vary as a function of TE for the two contrasts. In figure 1a, we show this in the form of activation maps, where significant activation is obtained at shorter echo times (TE=6.8 and 18 ms) for the MT-on experiment but not for the equivalent TEs in the MT-off experiment. To elucidate further these changes in activation, we took the MT-off$_{TE=28}$ activation map as a gold standard and used it to define the activated region of interest (ROI). Figure 1b shows the mean z-scores of activated voxels within this region as a measure of functional

sensitivity, as well as the total number of significantly activated voxels (both thresholded at z>2.3). With MT-on, we obtain the highest z-scores at the shortest TE and obtain similar numbers of activated voxels and z-scores at all TEs. In comparison, the MT-off experiment shows the typical behaviour of BOLD contrast, showing significant activation only at TE=28 ms.

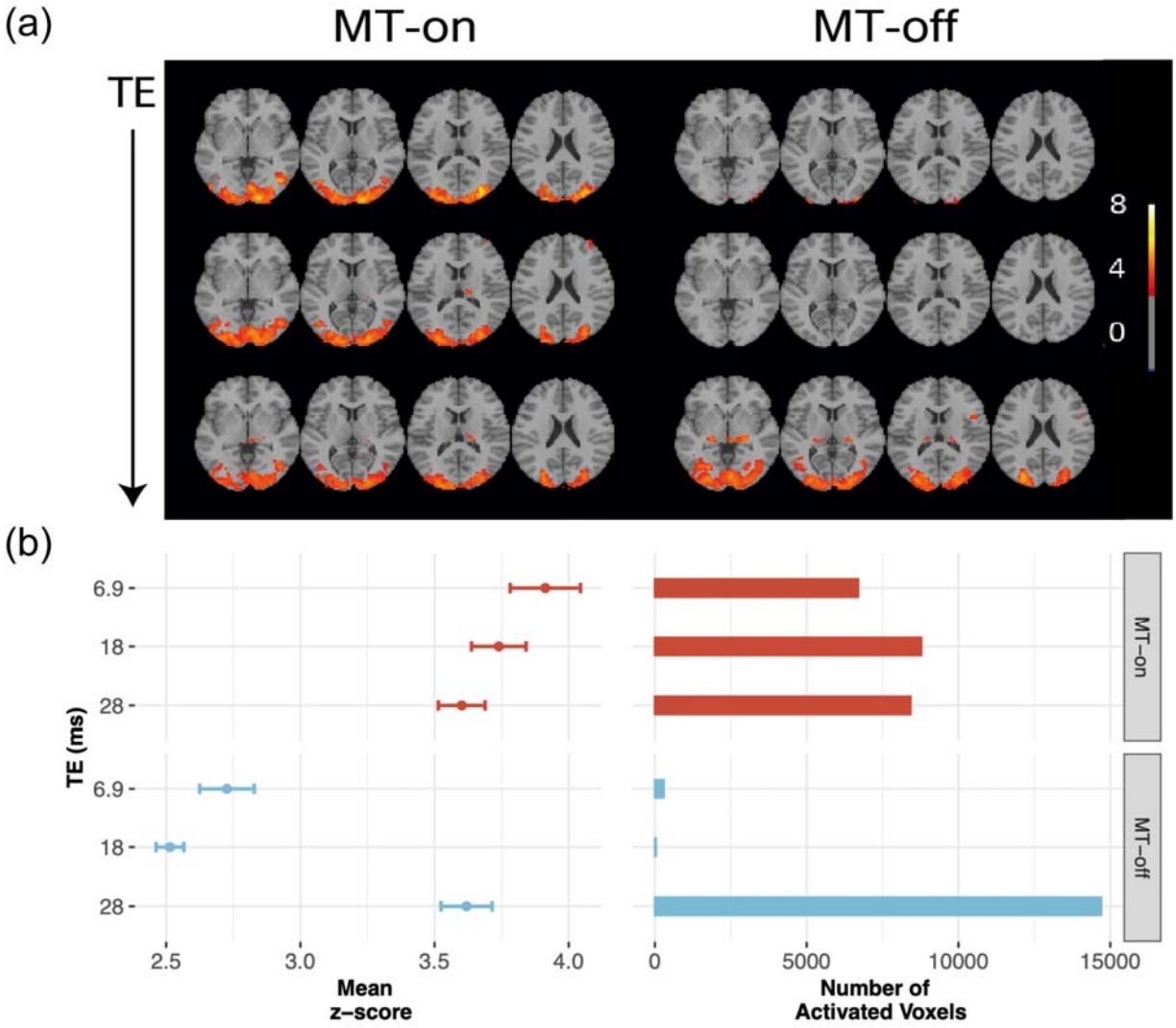

Figure 1: a) Group-level activation maps within the visual cortex covering four slices, for all three TE-values (6.9/18/28ms). All echo times show MT-on activation, whereas there is no statistically relevant activation for MT-off, except at TE=28ms showing BOLD contrast. b) Mean z-scores and the number of activated voxels within the region of interest defined by the MT-off$_{TE=28}$

activation map. The mean z-scores are calculated only for those pixels showing significant activation. Similar z-scores values are obtained for MT-on$_{TE=6.9}$ (3.9 ± 0.1) and MT-off$_{TE=28}$ (3. 6± 0.09), but there are more activated voxels for MT-off$_{TE=28}$.

We compared the relative sensitivity of the MT-on$_{TE=6.9}$ acquisition to the three MT-off acquisitions as a function of TE: the results are summarised in figure 2. The BOLD contrast at MT-off$_{TE=28}$ was used as a mask to exclude irrelevant areas. Only statistically significant differences are shown (fig. 2a). The left figure shows that at the shortest TE, MT-on displays overwhelmingly more activation than MT-off, despite eliminating more than half the native signal through the application of MT. The right figure shows that there are regions where MT-off$_{TE=28}$ shows greater activation than MT-on$_{TE=6.9}$. To understand the origin of this contrast better, we generated contour maps of the z-scores, superimposed on the early visual cortex, *i.e.,* within the region expected to show the strongest activation for the visual stimulus used. Figure 2b shows that the activation for MT-on$_{TE=6.9}$ is tightly localised to this region, whereas for MT-off$_{TE=28}$ extends beyond it, giving rise to the pattern shown on the right of fig. 2a. We also examined individual beta values within the ROI as a metric for activation strength and their distribution over subjects (fig 2c). This shows that the narrower distribution of beta values over subjects, i.e., lower inter-subject variability, is primarily responsible for the higher z-scores obtained for MT-on$_{TE=6.9}$.

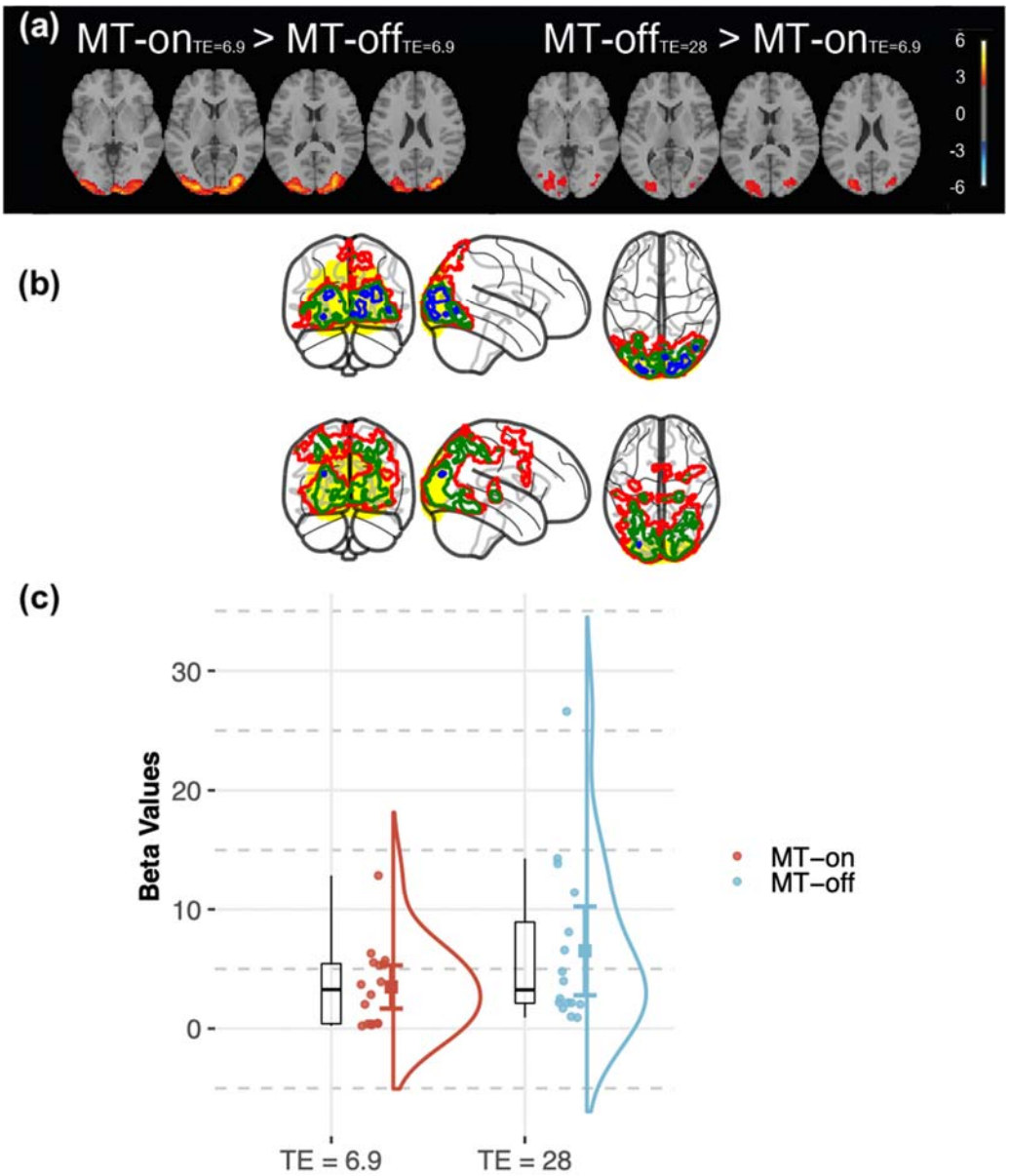

Figure 2: a) The group-level visual activation z-score maps are shown for the paired t-test at ($p < 0.05$) for the contrasts MT-on$_{TE=6.9}$ >MT-off$_{TE=6.9}$, and MT-off$_{TE=28}$ >MT-on$_{TE=6.9}$. b) Group-level activation maps for MT-on$_{TE=6.9}$ (top) and MT-off$_{TE=28}$ (bottom) showing contours in the z-score on a glass-brain (*https://nilearn.github.io*) *at z=3 (red), z=4 (green), and z=5 (blue) overlaid on the anatomically defined early visual cortex from Harvard-Oxford atlas (http://www.fmrib.ox.ac.uk/fsl/) in yellow. c) Average beta values across subjects masked by*

BOLD contrast at MT-off$_{TE=28}$ (dots). Boxplots show the median, 25th, and 75th percentiles. The error bars in the colour plots give the mean ± 95% confidence interval: MT-on$_{TE=6.9}$ (3.4 ± 1.8); MT-off$_{TE=28}$ (6.5 ± 3.7) . The distribution of individual beta values is plotted in the rightmost profiles.

Discussion

These results provide convincing evidence for an underlying contrast mechanism that differs from BOLD. This argument is based on: how the statistical maps vary as a function of TE; the different spatial distribution of the activation; and the different between-subject variance. For BOLD, the z-scores increase with TE as expected, with the maximum recorded at TE=28 ms, and no significant activation at the earlier echo times. For MT-on, the pattern of mean z-scores and numbers of activated voxels recorded with MT-on is consistent with reduced ABC and increased BOLD contributions, as TE increases. Although BOLD activates more voxels, the spatial distribution of MT-on$_{TE=6.9}$ is tightly localised to the early visual cortex. The distribution of beta-values for BOLD is also broader, and the corresponding z-values slightly smaller than for MT-on$_{TE=6.9}$.

The most plausible mechanism for the additional signal change is that it is driven by changes in CBV in the arterioles and capillaries. The estimated extravascular contribution to BOLD at 3T is 67%[26] and 70%.[27] Hence, removing roughly half the signal from grey matter will reduce the BOLD to about 65% of its original value. The MT pulses are not slice selective, and in the present work are transmitted via the body coil, and hence trivial explanations such as inflow can be excluded. By reducing the signal intensity by a factor of two, we reduce the non-BOLD physiological noise by the same factor, and the BOLD noise by about 35%. However, a reduction in noise level of itself cannot explain the qualitative changes in behaviour that we

observe. Hence, the differences in signal behaviour as a function of TE speak strongly to the proposed ABC mechanism.

Our approach relies on two hitherto unexplored aspects of MT as applied to functional neuroimaging: pulsed MT and minimal TE. We have implemented a pulsed MT-block prior to each excitation pulse, although a larger interval may be advantageous. [28] The time required for MT preparation is significantly shorter than needed for other methods that obtain blood volume weighted functional contrast.[3] In addition to the efficient MT contrast generation, the use of a short TE increases both sensitivity and efficiency. It also allows us to reduce or eliminate the signal dropouts that manifest at long TE in regions of poor static main field homogeneity and means that fMRI no longer falls in the category of fixed TE experiments, opening new possibilities for data acquisition, such as spiral trajectories[29-31] and short TE 3D-EPI.[32, 33] Although we chose the visual cortex for our initial implementation because of the strong activation that can be elicited in this region, there is no *a priori* reason to believe that our results are not applicable to the whole brain. ABC will have improved spatial localisation as it is mainly based on arterial CBV changes. Thus, high-resolution fMRI studies will benefit from a high ABC contribution to the functional contrast. Variations in MT efficiency through the brain (*c.f.* Figure S2) are far lower than the variation in T2*. Hence, by appropriate application of MT, all brain regions should become more equally accessible. As ABC is complementary to BOLD and straightforward to implement, we expect it to achieve widespread use in the near future.

Methods

MT On-resonance pulse

To suppress the tissue signal, a net 0° on-resonance MT preparation block[21] was implemented into the multi-echo EPI. The MT preparation block consists of two non-selective binomial RF pulses of opposite phases and magnitudes in the proportions ±1/ ∓2/ ±1 (6 ms). It is followed by a pseudo-random gradient spoiler scheme (3 ms) in all three directions (see figure 3a). The application of two binomial pulses back to back with inverted phase is aimed at reducing on-resonance signal attenuation, which could be related to transmit amplitude errors or large off-resonance effects due to static background field inhomogeneity.[34] Piloting showed that multiple repetitions of the dual-binomial MT pulse did not show any further improvement in MT image quality. The pseudo-random gradient was designed to avoid coherence pathways associated with the signal excited by the MT pulse (for example, fat signal). To achieve a constant steady state of continuous tissue suppression, the MT-block was played out before each slice excitation. The MT-flip angle pulse amplitude and pulse duration were optimized in a preliminary experiment to maximize the signal difference between CSF and tissue with respect to the specific absorption rate (SAR) limitations.

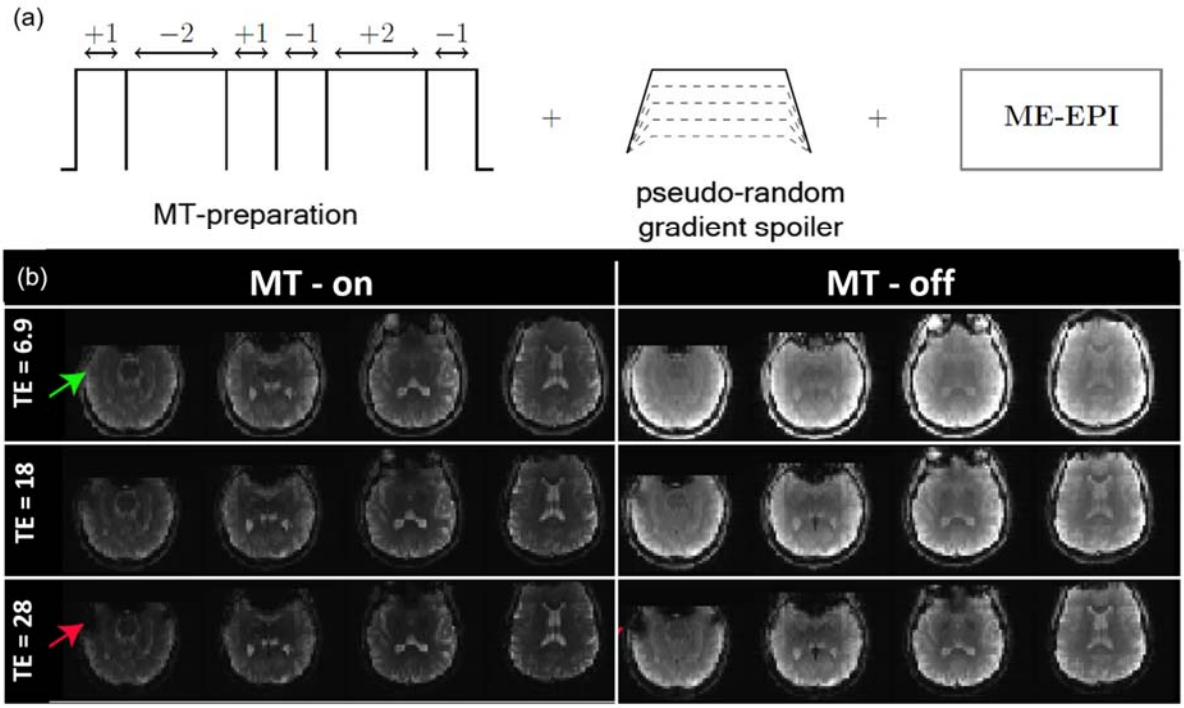

Figure 3: (a) Sequence design with the MT preparation module (6ms) and the pseudo-random gradient spoiler scheme (3ms) played out before every excitation of the ME-EPI sequence. (b) The image quality for MT-on and MT-off at different echoes. The green arrow indicates reduced dropout for MT-on$_{TE=6.9}$ as compared to MT-off$_{TE=28}$. Red arrows indicate dropout regions for MT-on/off$_{TE=28}$

Scanning protocols

The choice of protocols was determined based on preliminary experiments. [35, 36] The MT-pulse angle was adjusted empirically to maximally attenuate grey matter signal while restricting the attenuation of CSF to about 10%. We used the CSF signal attenuation in the ventricles, as a proxy for the arterial blood signal attenuation.

Data were acquired on a Siemens MAGNETOM Prisma (3T) MRI scanner (Erlangen, Germany) with a 32-channel head coil. The acquisition was based on a multi-echo gradient-echo EPI with MT-on and MT-off conditions. In the MT-on condition, the MT-block was implemented as explained above, whereas, in the MT-off condition, the RF-pulse of the MT-block was turned off

while the timing conditions remained the same. The MT flip angle for the MT-on acquisition was ±77°/∓154°/±77°. For both conditions, we acquired ME data at echo times TE=6.9/18/28ms. The first echo time was chosen to be as short as possible to maximise ABC in the MT-on condition. The upper limit was determined to ensure that a strong standard BOLD signal would be recorded, but that TR would not exceed 2s.

The acquisition protocol for the ME GE-EPI had the following parameters: in-plane resolution 3 mm isotropic and 38 slices without a gap for a coverage of 12 cm, Acquisition matrix 80x80, and fat saturation performed before each RF excitation. The flip angle for RF excitation was based on the Ernst angle of grey-matter (50°). The in-plane acceleration factor was three, with a partial Fourier factor of 6/8 and 2718 Hz/pixel acquisition bandwidth.

Anatomical scans were acquired for image registration using a sagittal 1 mm isotropic MP-RAGE with: TR of 2300 ms, TI of 900 ms, TE of 3 ms, FA 9°, turbo factor 16 and an in-plane acceleration factor of 2. The total acquisition time was 5:20min. All imaging sequences were automatically aligned using an auto-align localizer sequence.

Data Acquisition

The data quality using MT-on acquisition is shown in figure 3b, with uniform suppression of grey matter signal in the regions of activation (figure S2). We acquired ME-GE EPI data from 16 subjects (10M/6F 26 ± 6 yrs) with this number based on power analysis for a mixed-effects analysis at the group-level.[37] Pilot-data from two preliminary studies were used for the power calculation (three subjects (2M/1F 28 ± 4 yrs) and 7 subjects (3M/4F 25 ±4 yrs)).[35, 36] The power analysis was implemented in the fMRIpower software package (http://fmripower.org). This method estimates power for detecting significant activation within specific regions of interest, with the assumption that the planned studies will have the same number of runs per subject, runs of the same length, similar scanner noise characteristics, and data analysis with a comparable model. All power calculations were based on an atlas[38] and used a p-value

threshold of 0.005 for a one-sided hypothesis test. With 16 subjects, we predicted at least 80% power to detect an effect size of 0.7 in the Inferior Occipital Gyrus (IOG) with MT-on at TE of 6.9 ms and MT-off at TE=28 ms using mixed-effects analysis at the group-level.

The participants were shown a hemifield (R/L) checkerboard flickering at 4Hz randomly distributed across trials with a block design of [10s on, 26-32 off ISI]. During the entire task, the participants were asked to focus on the grey fixation cross in the middle of the screen and press the button box with the R/L index finger whenever the fixation cross changed colour using the immediately previous stimulus hemifield as a reference for R or L. The total duration of the task was 10 minutes. Stimuli were presented, and button presses were recorded using MATLAB 2018a, The MathWorks, Inc., Natick, Massachusetts, United States). Before performing the task in the scanner, participants practiced on a desktop computer located next to the scanning console to guarantee that the procedure was understood. Each subject performed two runs of ten minutes during a session with one MT-on and the other MT-off. This is because the lengthy duration required for the build-up of steady-state and decay of the MT effect makes it difficult to alternate in a single run. The order in which MT-on/off was applied was counterbalanced across subjects.

Functional Processing

Before data pre-processing, DICOMs were converted to NIfTI's using dcm2niix.[39] For each BOLD run, the following pre-processing was performed using FSL. First, head-motion parameters were estimated using a reference volume for the BOLD data (transformation matrices, and six corresponding rotation and translation parameters) using MCFLIRT.[40] The BOLD data were then co-registered to the T1w reference using FLIRT[41] with the boundary-based registration cost-function.[42] Co-registration was configured with nine degrees of freedom to account for distortions remaining in the BOLD reference. The BOLD data were resampled to

MNI152NLin2009cAsym to generate pre-processed BOLD data in standard space.[43, 44] These were smoothed with a 6mm kernel and high pass filtered with a cut-off frequency of 1/100s.

Data Analysis

MT-on and MT-off images were analyzed using FSL 6.0.1 to find the activation in: (1) right visual cortex for left hemifield stimulation, (2) left visual cortex for right hemifield, and (3) their combination for both hemifields. The datasets were analysed using FSL FEAT[45] to estimate the activation during the checkerboard task for all subjects and both conditions. The design matrix for the single-subject FEAT analysis modelled three explanatory variables (EV): (1) right hemifield trials vs. baseline, (2) left hemifield vs. baseline and finally (3) overlapping effects from right and left hemifield (R+L); each convolved with a hemodynamic response and constant term. Additionally, three contrasts were set up, one contrast, e.g., [1 0 0]] for each EV. The last contrast is important to look at the activation that would be consistent for both hemifields. To verify the hemodynamic convolution with regressors of interest for the MT-on data, the hemodynamic responses within the right and left hemifields were computed using the first-level parameter estimates, as shown in figure S2. The MT-on data showed a similar temporal evolution of the hemodynamic response as the BOLD contrast found for MT-off.

A second-level analysis was then carried out, with FEAT, using mixed-effects, which allows explicit modelling of both within- and between-subject variance components.[46]

To make inferences at the group level, a one-sided t-test was performed to assess the difference in z-scores. The z-score maps were thresholded at $z > 2.3$ at ($p < 0.05$, Family wise error (FWE) corrected). The t-test was conducted by concatenating parameter estimates from each contrast at the single-subject level.

Next, we performed a paired t-test at the significance level of ($p<005$) to detect statistically significant differences between each method. We compared the MT-on$_{TE=6.9}$ to the MT-off data at all three TEs.

Acknowledgements.

The authors would like to thank Peter Koopmans and Peter Hagoort for critical comments on this manuscript; Benedikt Ehinger and Floris de Lange for advice on stimulus design; and Christian Beckmann for advice on statistical analysis.

References

1. Rosen, B.R. & Savoy, R.L. fMRI at 20: has it changed the world? *Neuroimage* **62**, 1316-1324 (2012).
2. Ogawa, S., Lee, T., Nayak, A.S. & Glynn, P. Oxygenation-sensitive contrast in magnetic resonance image of rodent brain at high magnetic fields. *Magn. Reson. Med.* **14**, 68-78 (1990).
3. Lu, H., Golay, X., Pekar, J.J. & van Zijl, P.C.M. Functional magnetic resonance Imaging based on changes in vascular space occupancy. *Magn. Reson. Med.* **50**, 263-274 (2003).
4. Lu, H.Z., Golay, X., Pekar, J.J. & van Zijl, P.C.M. Sustained poststimulus elevation in cerebral oxygen utilization after vascular recovery. *Journal of Cerebral Blood Flow and Metabolism* **24**, 764-770 (2004).
5. Stefanovic, B. & Pike, G.B. Venous refocusing for volume estimation: VERVE functional magnetic resonance imaging. *Magn. Reson. Med.* **53**, 339-347 (2005).
6. Huber, L. et al. Slab-selective, BOLD-corrected VASO at 7 Tesla provides measures of cerebral blood volume reactivity with high signal-to-noise ratio. *Magn Reson Med* **72**, 137-148 (2014).
7. Huber, L. et al. Functional cerebral blood volume mapping with simultaneous multi-slice acquisition. *Neuroimage* **125**, 1159-1168 (2016).
8. Huber, L. et al. High-Resolution CBV-fMRI Allows Mapping of Laminar Activity and Connectivity of Cortical Input and Output in Human M1. *Neuron* **96**, 1253-1263.e1257 (2017).
9. Qiu, D., Zaharchuk, G., Christen, T., Ni, W.W. & Moseley, M.E. Contrast-enhanced functional blood volume imaging (CE-fBVI): Enhanced sensitivity for brain activation in

humans using the ultrasmall superparamagnetic iron oxide agent ferumoxytol. *Neuroimage* **62**, 1726-1731 (2012).

10. D'Arceuil, H. et al. Ferumoxytol enhanced resting state fMRI and relative cerebral blood volume mapping in normal human brain. *Neuroimage* **83**, 200-209 (2013).
11. Baumgartner, R. et al. Evaluation of an fMRI USPIO-based assay in healthy human volunteers. *Journal of Magnetic Resonance Imaging* **46**, 124-133 (2017).
12. Jin, T. & Kim, S.G. Improved cortical-layer specificity of vascular space occupancy fMRI with slab inversion relative to spin-echo BOLD at 9.4 T. *Neuroimage* **40**, 59-67 (2008).
13. Jin, T. & Kim, S.G. Cortical layer-dependent dynamic blood oxygenation, cerebral blood flow and cerebral blood volume responses during visual stimulation. *Neuroimage* **43**, 1-9 (2008).
14. Balaban, R.S., Chesnick, S., Hedges, K., Samaha, F. & Heineman, F.W. Magnetization transfer contrast in MR imaging of the heart. *Radiology* **180**, 671-675 (1991).
15. Wolff, S.D. & Balaban, R.S. Magnetization Transfer Contrast (MTC) and Tissue Water Proton Relaxation in Vivo. *Magn. Reson. Med.* **10**, 135-144 (1989).
16. Zhou, J.Y., Payen, J.F. & van Zijl, P.C.M. The interaction between magnetization transfer and blood-oxygen-level-dependent effects. *Magn. Reson. Med.* **53**, 356-366 (2005).
17. Kim, T., Hendrich, K. & Kim, S.G. Functional MRI with Magnetization Transfer Effects: Determination of BOLD and Arterial Blood Volume Changes. *Magn. Reson. Med.* **60**, 1518-1523 (2008).
18. Kim, T. & Kim, S.G. Quantification of cerebral arterial blood volume and cerebral blood flow using MRI with modulation of tissue and vessel (MOTIVE) signals. *Magn. Reson. Med.* **54**, 333-342 (2005).

19. Song, A.W., Wolff, S.D., Balaban, R.S. & Jezzard, P. The effect of off-resonance radiofrequency pulse saturation on fMRI contrast. *NMR in Biomedicine* **10**, 208-215 (1997).

20. Zhang, R.Y., Cox, R.W. & Hyde, J.S. The effect of magnetization transfer on functional MRI signals. *Magn. Reson. Med.* **38**, 187-192 (1997).

21. Pike, G.B., Hu, B.S., Glover, G.H. & Enzmann, D.R. Magnetization transfer time-of-flight magnetic-resonance angiography. *Magn. Reson. Med.* **25**, 372-379 (1992).

22. Krieger, S.N., Streicher, M.N., Trampel, R. & Turner, R. Cerebral blood volume changes during brain activation. *Journal of Cerebral Blood Flow and Metabolism* **32**, 1618-1631 (2012).

23. Cai, K.J., Haris, M., Singh, A., Li, L.Z. & Reddy, R. in Oxygen Transport to Tissue Xxxiv, Vol. 765. (eds. W.J. Welch, F. Palm, D.F. Bruley & D.K. Harrison) 31-37 (2013).

24. Sakadzic, S. et al. Large arteriolar component of oxygen delivery implies a safe margin of oxygen supply to cerebral tissue. *Nature communications* **5** (2014).

25. Menon, R.S., Ogawa, S., Tank, D.W. & Ugurbil, K. 4 Tesla gradient recalled echo characteristics of photic stimulation-induced signal changes in the human primary visual cortex. *Magn Reson Med* **30**, 380-386 (1993).

26. Lu, H. & Van Zijl, P.C.M. Experimental measurement of extravascular parenchymal BOLD effects and tissue oxygen extraction fractions using multi-echo VASO fMRI at 1.5 and 3.0 T. *Magn. Reson. Med.* **53**, 808-816 (2005).

27. Donahue, M.J. et al. Blood oxygenation level-dependent (BOLD) total and extravascular signal changes and ΔR2* in human visual cortex at 1.5, 3.0 and 7.0 T. *NMR in Biomedicine* **24**, 25-34 (2011).

28. Helms, G. & Piringer, A. Simultaneous measurement of saturation and relaxation in human brain by repetitive magnetization transfer pulses. *NMR in Biomedicine* **18**, 44-50 (2005).

29. Yang, Y.H. et al. Fast 3D functional magnetic resonance imaging at 1.5 T with spiral acquisition. *Magn. Reson. Med.* **36**, 620-626 (1996).

30. Lai, S. & Glover, G.H. Three-dimensional spiral fMRI technique: A comparison with 2D spiral acquisition. *Magn. Reson. Med.* **39**, 68-78 (1998).

31. Anderson, A.G., Wang, D.H. & Pipe, J.G. Controlled aliasing for improved parallel imaging with a 3D spiral staircase trajectory. *Magn. Reson. Med.*

32. Poser, B.A., Koopmans, P.J., Witzel, T., Wald, L.L. & Barth, M. Three dimensional echo-planar imaging at 7 Tesla. *Neuroimage* **51**, 261-266 (2010).

33. Narsude, M., Gallichan, D., van der Zwaag, W., Gruetter, R. & Marques, J.P. Three-dimensional echo planar imaging with controlled aliasing: A sequence for high temporal resolution functional MRI. *Magn Reson Med* **75**, 2350-2361 (2016).

34. Davies, N.P., Summers, I.R. & Vennart, W. Optimum setting of binomial pulses for magnetization transfer contrast. *Jmri-Journal of Magnetic Resonance Imaging* **11**, 539-548 (2000).

35. Schulz, J., Fazal, Z., Metere, R., Marques, J.P. & Norris, D.G. in International Society for Magnetic Resonance in Medicine (Paris; 2020).

36. Schulz, J., Fazal, Z., Metere, R., Marques, J.P. & Norris, D.G. in Organisation for Human Brain Mapping (2020).

37. Mumford, J.A. & Nichols, T.E. Power calculation for group fMRI studies accounting for arbitrary design and temporal autocorrelation. *Neuroimage* **39**, 261-268 (2008).

38. Tzourio-Mazoyer, N. et al. Automated anatomical labeling of activations in SPM using a macroscopic anatomical parcellation of the MNI MRI single-subject brain. *Neuroimage* **15**, 273-289 (2002).

39. Li, X., Morgan, P.S., Ashburner, J., Smith, J. & Rorden, C. The first step for neuroimaging data analysis: DICOM to NIfTI conversion. *Journal of Neuroscience Methods* **264**, 47-56 (2016).

40. Jenkinson, M., Bannister, P., Brady, M. & Smith, S. Improved Optimization for the Robust and Accurate Linear Registration and Motion Correction of Brain Images. *Neuroimage* **17**, 825-841 (2002).

41. Jenkinson, M. & Smith, S. A global optimisation method for robust affine registration of brain images. *Medical image analysis* **5**, 143-156 (2001).

42. Greve, D.N. & Fischl, B. Accurate and robust brain image alignment using boundary-based registration. *Neuroimage* **48**, 63-72 (2009).

43. Fonov, V. et al. Unbiased average age-appropriate atlases for pediatric studies. *Neuroimage* **54**, 313-327 (2011).

44. Fonov, V., Evans, A., McKinstry, R., Almli, C. & Collins, D. Unbiased nonlinear average age-appropriate brain templates from birth to adulthood. *Neuroimage* **47**, S102 (2009).

45. Woolrich, M.W., Ripley, B.D., Brady, M. & Smith, S.M. Temporal Autocorrelation in Univariate Linear Modeling of FMRI Data. *Neuroimage* **14**, 1370-1386 (2001).

46. Beckmann, C.F., Jenkinson, M. & Smith, S.M. General multilevel linear modeling for group analysis in FMRI. *Neuroimage* **20**, 1052-1063 (2003).